PALEOCEANOGRAPHY, VOL. 15, NO. 1, PAGES 95-109, FEBRUARY 2000

Sea-surface temperatures of the southwest Pacific Ocean during the Last Glacial Maximum

T. T. Barrows,[1] S. Juggins,[2] P. De Deckker,[3] J. Thiede,[4] and J. I. Martinez[5]

Abstract. The southwest Pacific Ocean covers a broad range of surface-water conditions ranging from warm, salty water in the subtropical East Australian Current to fresher, cold water in the Circumpolar Current. Using a new database of planktonic foraminifera assemblages (AUSMAT-F2), we demonstrate that the modern analog technique can be used to accurately reconstruct the magnitude of sea-surfacetemperature (SST) in this region. We apply this technique to data from 29 deep-sea cores along a meridional transect of the southwest Pacific Ocean to estimate the magnitude of SST cooling during the Last Glacial Maximum. We find minimal cooling in the tropics (0°-2°C), moderate cooling in the subtropical midlatitudes (2°-6°C), and maximum cooling to the southeast of New Zealand (6°-10°C). The magnitude of cooling at the sea surface from the tropics to the temperate latitudes is found to generally be less than cooling at the surface of adjacent land masses.

1. Introduction

The southwest Pacific Ocean, including its marginal seas, covers a broad region from the tropical Coral Sea to the subantarctic Southern Ocean (Figure 1). Sea-surface temperatures (SST) range from more than 28°C in the northern Coral Sea during the austral summer to less than 10°C in the southern Tasman Sea during the austral winter [*Levitus and Boyer*, 1994]. The temperature of the ocean surface is central to understanding the oceanography and climates of the southwest Pacific Ocean, as it is directly related to the Walker Circulation, El Niño-Southern Oscillation, the position of the Intertropical Convergence Zone, hemispheric circulation, and cyclonogenesis. Thus it is an important parameter in paleoceanography when assessing the magnitude of climate change through time, particularly within a glacial-interglacial cycle.

The Last Glacial Maximum (LGM) represents a key climatic end-member in Quaternary studies, being the most recent example of a full glaciation and having the best preserved and dated records. A long-standing paradox in Quaternary climate studies centers around the apparent conflict between the magnitude of cooling at the tropical sea surface and adjacent land surfaces at the LGM [*Webster and Streten*, 1978; *Rind and Peteet*, 1985]. The equatorial western Pacific has been a focus of debate since the Climate: Long-Range Investigation, Mapping and Prediction project (CLIMAP) [*CLIMAP Project Members*, 1976, 1981; *Moore et al.*, 1980] suggested that the tropical sea surface did not cool by a significant amount during the LGM. This conflicts with glacial evidence from New Guinea suggesting cooling at high elevations of 5°-6°C [*Löffler*, 1982]. Additionally, CLIMAP reconstructed a warm anomaly off the eastern coast of Australia and suggested that the western boundary circulation was even stronger than present. A similar conflict between the magnitude of SST and land-surface temperature cooling at the LGM occurs beyond the tropics in midlatitude southern Australia, where continental evidence shows cooling of up to 9°C from present values [*Galloway*, 1965; *Miller et al.*, 1997] compared to *CLIMAP Project Members* [1981] estimates showing only 2°-3°C of cooling around the southeast margin of Australia.

CLIMAP reconstructed SST using a series of multifactor transfer functions relating planktonic foraminiferal assemblages to SST [*Imbrie and Kipp*, 1971] and developed separate predictive equations for each ocean. *Prell* [1985] refined this approach using the modern analog technique (MAT), basing SST estimates on an extensive analog database containing many of the same core tops used in the CLIMAP equations. Applying the MAT to the original CLIMAP data, *Prell* [1985] derived similar tropical and subtropical cooling to *CLIMAP Project Members* [1981]. *Anderson et al.* [1989] and *Thunell et al.* [1994] later reinvestigated the Coral and Tasman Seas using the MAT and new cores. The minimal SST cooling in the tropics was reproduced, but *Anderson et al.* [1989] found that the warm anomaly drawn by *CLIMAP Project Members* [1981] was due to a single core that had poor stratigraphic control.

Recently, there has been a return to using original CLIMAP transfer functions in the southwest Pacific Ocean, despite *Prell* [1985] showing that the MAT outperforms these equations. *Wells and Connell* [1997] and *Wells and Okada* [1997] have applied the Indian Ocean transfer function, the Northern Pacific Ocean transfer function, and the MAT [*Prell*, 1985] to cores from west of Tasmania to east of New Zealand. Additionally, *Weaver et al.* [1998] have applied the North Atlantic transfer function to a set of high-quality cores from the eastern margin of New Zealand. *Nelson et al.* [1994] have also attempted to estimate SST changes using a separate technique based on oxygen-isotope records from cores in the same area

[1]Research School of Earth Sciences, The Australian National University, Canberra, ACT, Australia.
[2]Department of Geography, University of Newcastle, Newcastle upon Tyne, England, United Kingdom.
[3]Geology Department, The Australian National University, Canberra, ACT, Australia.
[4]Alfred-Wegener-Institut für Polar- und Meeresforschung, Bremerhaven, Germany.
[5]Departamento de Geología, Universidad EAFIT, Medellín, Colombia.

Paper number 1999PA900047.
0883-8305/00/1999PA900047$12.00

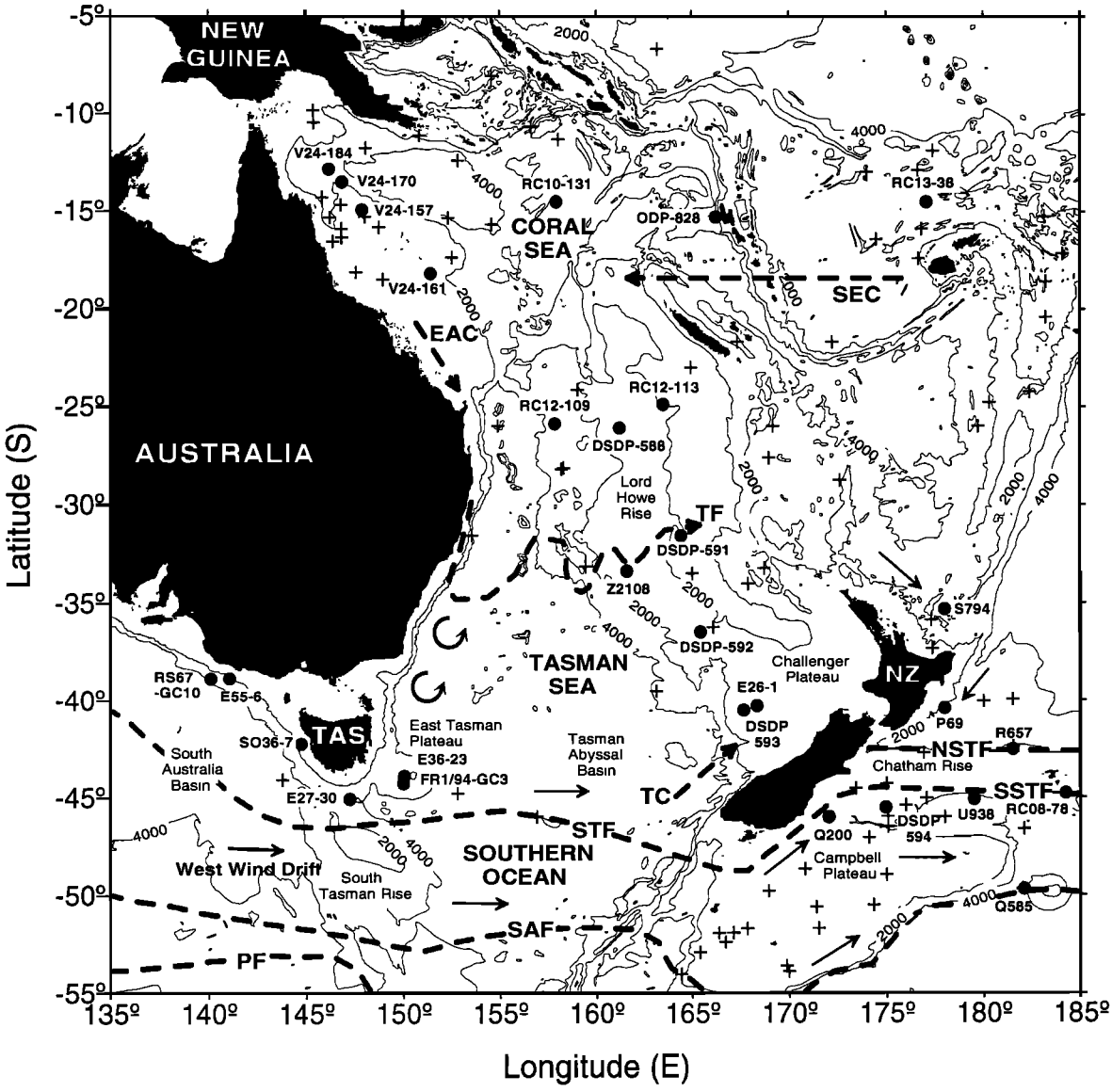

Figure 1. Regional surface oceanography of the southwest Pacific Ocean showing major fronts and currents. Depending upon conditions, the TF either continues out into the open South Pacific or continues around the northern tip of New Zealand. The modal TF position shown here is from *Mulhearn* [1987]. STF, SAF, and PF positions are from *Belkin and Gordon* [1996] and the SEC position is from *Tomczak and Godfrey* [1994]. Arrows indicate generalized directions of surface currents, and the bathymetric contour interval is 2000 m. Solid circles indicate the location of cores used in the Last Glacial Maximum reconstruction, and crosses indicate positions of core tops used in the test database (SEC, South Equatorial Current; EAC, East Australian Current; TF, Tasman Front; TC, Tasman Current; STF, Subtropical Front; NSTF, Northern STF; SSTF, Southern STF; SAF, Subantarctic Front; PF, Polar Front; NZ, New Zealand; TAS, Tasmania).

and found minor glacial-interglacial changes. Independently of SST estimates, other research in the region since *CLIMAP Project Members* [1981] has sought to describe the changing distribution of surface water masses and frontal systems between the LGM and the Holocene [*Martinez*, 1994; *Passlow et al.*, 1997]. These studies have suggested that the Subtropical Front (STF) has moved little between the LGM and present.

The possibility that SST cooling was minimal and that the STF is rather static in the southwest Pacific Ocean sector during the LGM implies that this region is relatively insensitive to climate change. The difference in cooling between land and sea surface also appears paradoxical. In this paper, we seek to reevaluate techniques used in the southwest Pacific Ocean to estimate SST using planktonic foraminifera and oxygen-isotope analyses. We then use new and existing faunal and isotope records to revise estimates of SST during the LGM to determine any meridional or zonal shifts in isotherms during the LGM. Finally, we compare these estimates to the degree of cooling over adjacent land masses.

2. Modern Oceanography

The southwest Pacific Ocean covers a wide range of water masses and surface currents (Figure 1). Surface water in the Coral Sea typically has very high SST (warmest month >28°C) with low seasonality and is derived from the South Equatorial Current [*Tomczak and Godfrey*, 1994]. The East Australian Current (EAC), a western boundary current, transfers a significant amount of heat poleward from the Coral Sea and forms the western limb of the South Pacific subtropical gyre. The Subtropical Surface Water in the EAC derives its characteristics from high insolation and evaporation in the middle latitudes and is consequently warm and saline [*Garner*, 1959]. The EAC has a significant influence on the coastal weather, supporting warm and moist climates along the east coast of Australia. The Tasman Front marks the contact where about half the volume of the EAC moves eastward as a zonal jet from the coast of Australia at ~34°S across the Tasman Sea [*Stanton*, 1979, 1981]. The Tasman Front lies under the the axis of the subtropical high-pressure ridge and experiences the highest seasonality in the Tasman Sea because of seasonal shifts in its position. Farther south, warm-cored eddies from the East Australian Current continue down the coast [*Nilsson and Cresswell*, 1981; *Cresswell and Legeckis*, 1986]. There is some return flow of Subtropical Surface Water to the west of New Zealand as the Tasman Current [*Heath*, 1985].

The Subtropical Surface Water converges with cooler, less saline Subantarctic Surface Water at the southern extremity of the EAC eddy field at the Subtropical Front (STF) [*Orsi et al.*, 1995]. This major water-mass boundary is a zone broadly located around 45°-47°S south of Tasmania to New Zealand, extends along the east coast of the South Island of New Zealand as the Southland Front, and splits into two fronts along the Chatham Rise [*Heath*, 1985; *Belkin and Gordon*, 1996]. The STF marks a zone of rapid north-south decrease in temperature and salinity and increase in dissolved nutrients, such as nitrate and phosphate. The STF is approximated by the 34.8-35.1 isohalines, the ~10°C winter, and the ~15°C summer isotherms in the southern Tasman Sea [*Garner*, 1959]. Subantarctic Surface Water south of the STF is driven eastward by the prevailing westerly winds as part of the Circumpolar Current.

In the Southern Ocean the Antarctic Polar Frontal Zone lies between ~50° and 60°S and is bounded in the north by the Subantarctic Front and by the Polar Front in the south. The Subantarctic Front forms the boundary between the Australasian Subantarctic Surface Water and the Circumpolar Subantarctic Surface Water [*Heath*, 1985]. The Subantarctic Front is defined by the presence of the intermediate S_{min} and the Subantarctic Mode Water thermostad to its north [*Belkin and Gordon*, 1996]. The Polar Front (also known as the Antarctic Convergence) is presently characterized by the northern terminus of the subsurface T_{min} layer and the vertical 2°C isotherm in winter [*Belkin and Gordon*, 1996].

3. Methods for Evaluation of Techniques

Six separate techniques using planktonic foraminifera have been applied in the southwest Pacific to estimate past SST, producing variable results when applied to the same data [*Prell*, 1985; *Wells and Okada*, 1997]. These include the Tasman Sea transfer function (FP4 [*Thiede, et al.*, 1997]), the equatorial-northern Pacific Ocean transfer function (FP12E [*Thompson*, 1981]), the Indian Ocean transfer function (FI-2 [*Hutson and Prell*, 1981]), the Atlantic Ocean transfer function (FA-20RSC [*Molfino et al.*, 1982]), the MAT using a Pacific Ocean or global database [*Prell*, 1985], and the oxygen-isotopic composition of planktonic foraminifera [following *Emiliani*, 1955]. To evaluate the ability of these techniques to accurately estimate SST in the southwest Pacific Ocean, we applied them to a test database of 106 core tops constructed from published data for the southwest Pacific Ocean [*Anderson*, 1995; *Thiede et al.*, 1997; *Weaver et al.*, 1997]. This database covers a wide range of SSTs (1.5°-29.8°C), water depths (428 - 4709 m), and foraminferal dissolution states. We also test the MAT using AUSMAT-F2, a modified and expanded version of the *Prell* [1985] global database, developed to provide more accurate SST estimates in the Southern Hemisphere [*T.T. Barrows, manuscript in preparation*, 1999]. AUSMAT-F2 represents an update from a previous version (AUSMAT-F1, used by *Martinez et al.* [1999a] and *Martinez et al.* [1999b]), as it now includes ~500 new core tops, mostly from published material for Australasian waters, bringing the database to a total of 1091 core tops.

Reconstructions for the factor-analysis transfer functions follow the approach of *Imbrie and Kipp* [1971]. The FP4B equation used here represents an update from that presented by *Thiede et al.* [1997], as we calibrated it using the SST database of *Levitus and Boyer* [1994]. For the MAT we used the squared chord distance as the dissimilarity measure, and each estimate was the weighted mean of the best 10 analogs (*Prell* [1985]; global database) or 12 analogs (AUSMAT-F2 database). When calculating the distance coefficient, subvarieties of *Globigerinoides ruber*, *Globigerinoides sacculifer*, and *Globorotalia menardii* were grouped together, and unidentified taxa were excluded. The taxonomy of the assemblage from each core top was adjusted for use in each transfer function and the modern analog database.

To test the applicability of using the oxygen-isotopic composition of *Globigerina bulloides* as a technique for estimating mean annual SST, we recalculated modern SST estimates from 32 core top samples published by *Weaver et al.* [1997] (Table 1, Appendix A). Modern $\delta^{18}O$ of the surface seawater was estimated using an equation relating isotopic composition with surface salinity in the south Pacific Ocean [*Craig and Gordon*, 1965]. Salinity was determined using annual sea-surface data from *Levitus et al.* [1994]. To relate temperature to isotopic fractionation, we applied the 12-chamber *G. bulloides* relationship calculated from cultured specimens [*Bemis et al.*, 1998] and two other equations based on culturing experiments on planktonic foraminifera: *Orbulina universa* [*Bemis et al.*, 1998] and *Globigerinoides sacculifer* [*Erez and Luz*, 1983].

The performance of each technique was measured using four parameters: the squared correlation coefficient r^2, root-mean-squared error of prediction (RMSEP), average bias, and maximum bias. The squared correlation coefficient measures the strength of the relationship between the observed and inferred SST, while the RMSEP gives an overall measure of the predictive ability [*Wallach and Goffinet*, 1989]. The average bias indicates systematic errors across the whole data set, and the

Table 1. Performance of Sea-Surface Temperature Estimation Techniques

	Transfer Functions								Modern Analog Technique				$\delta^{18}O$			
	FP4B		FP12E		FI-2		FA20RSC		Prell [1985]		AUSMAT-F2		*G. bull.*	*O. uni.*	*G. sacc.*
Statistics	Warm	Cold	Warm	Cold	Warm	Cold	Warm	Cold	Warm	Cold	T_0max	T_0min	T_0ann	T_0ann	T_0ann
maximum	29.5	29.0	30.0	29.0	28.6	29.2	28.9	27.1	30.3	29.2	30.4	29.2	25	25	30
minimum	19.2	9.5	12.0	3.0	3.0	1.0	3.0	0.0	1.0	0.0	0.9	-2.0	15	15	14
r^2	0.51	0.65	0.86	0.91	0.96	0.92	0.96	0.94	0.96	0.95	0.99	0.98	0.89	0.89	0.89
RMSEP	5.8	4.9	5.9	3.3	2.0	2.7	1.8	2.3	2.1	1.9	0.9	1.0	7.5	4.3	3.2
Mean Bias	2.5	2.1	4.3	1.9	-1.3	-1.7	-0.9	-1.5	-1.1	-0.6	-0.1	-0.1	-7.1	-3.6	-2.5
Max Bias	36.4	29.3	11.3	4.8	-3.2	-4.2	-1.9	-4.2	-3.0	-2.4	-1.2	-2.0	-9.7	-6	-3.9

Abbreviations are as follows (see text for further explanation): minimum, and maximum, temperature minimum or maximum of original calibration dataset; RMSEP, root-mean-squared error of prediction; warm, cold, February and August temperatures at the sea surface; T_0max, T_0min, temperatures of the warmest and coolest months at the sea-surface; T_0ann, mean annual temperature at the sea surface; *G. bull.*, *Globigerina bulloides*; *G. sacc.*, *Globigerinoides sacculifer*; *O. uni.*, *Orbulina universa*.

maximum bias measures the tendency to overestimate or underestimate along particular parts of the SST gradient [*ter Braak and Juggins*, 1993].

4. Results and Discussion

Results from the peformance evaluation are summarized in Table 1 and Figure 2. The individual estimates are listed in Appendix A[1] . Estimates of SST based on the factor-analysis transfer functions demonstrate considerable performance variation between equations. Tasman Sea equation FP4B performs well at SSTs above 10°C (cold equation) but grossly overestimates SSTs below this, giving an overall large RMSEP. The Pacific Ocean equation FP12E grossly overestimates warmest month SST over the whole temperature range. The Indian Ocean equation FI-2 systematically underestimates both February and August SST. The Atlantic Ocean equation FA20RSC performs well in the Pacific Ocean [*Prell*, 1985; *Weaver et al.*, 1997] and produces reasonable results when applied to the test data set used here. The lack of fit between the core top assemblages and each factor model is indicated in Appendix A by the sample communalities, with values <0.8 taken to indicate assemblages that are poorly modeled by the factor equations. Given their poor performance, it is not surprising that very low communalities are recorded for FP4B and FP12E, suggesting that these equations are unable to model many of the faunal associations recorded in the test core tops. Communalities are generally higher for FI2 and FA20RSC, but a significant number of test core tops also lack close faunal association with these factor models.

Estimates from the modern analog technique also show variable quality depending on the analog database used. Estimates using *Prell*'s [1985] global database systematically underestimate observed SST with high error in the middle of the temperature range, whereas the AUSMAT-F2 database produces the lowest values for both prediction error (0.9° and 1.0°C for T_0max and T_0min respectively) and average bias (-0.1°C). A goodness-of-fit measure for the analog methods is given by the minimum squared chord distance (MSCD), representing the distance of each test sample to its closest modern analog. For the Prell database, 21 of the 106 test core tops have a MSCD >0.2, indicating that one fifth lack good analogs in this database. For the AUSMAT-F2 database, all MSCDs are <0.2 and only 10 are >0.1, indicating that all test assemblages have close faunal analogs in this database. A test of reproducibility is provided by the comparison of estimates from eight duplicate core tops in the test database, the taxonomy performed by separate workers [*Anderson*, 1995; *Thiede et al.*, 1997]. The duplicates differ by an average of only 0.1° and 0.2°C (T_0max and T_0min, respectively) when estimated with AUSMAT-F2, whereas they differ by 0.7° and 1.2°C (warm and cold seasons, respectively) using the *Prell* [1985] database, indicating the MAT using AUSMAT-F2 is somewhat more resistant to differences in taxonomy.

[1]Supporting Appendices A and B are available electronically at the World Data Center A for Paleoclimatology, NOAA/NGDC, 325 Broadway, Boulder, Colorado (email: paleo@noaa.ngdc.gov; URL: http://www.ngdc.noaa.gov/paleo) and at the Australian Quaternary Data Archive (URL: http://rses.anu.edu.au/enproc/AQUADATA).

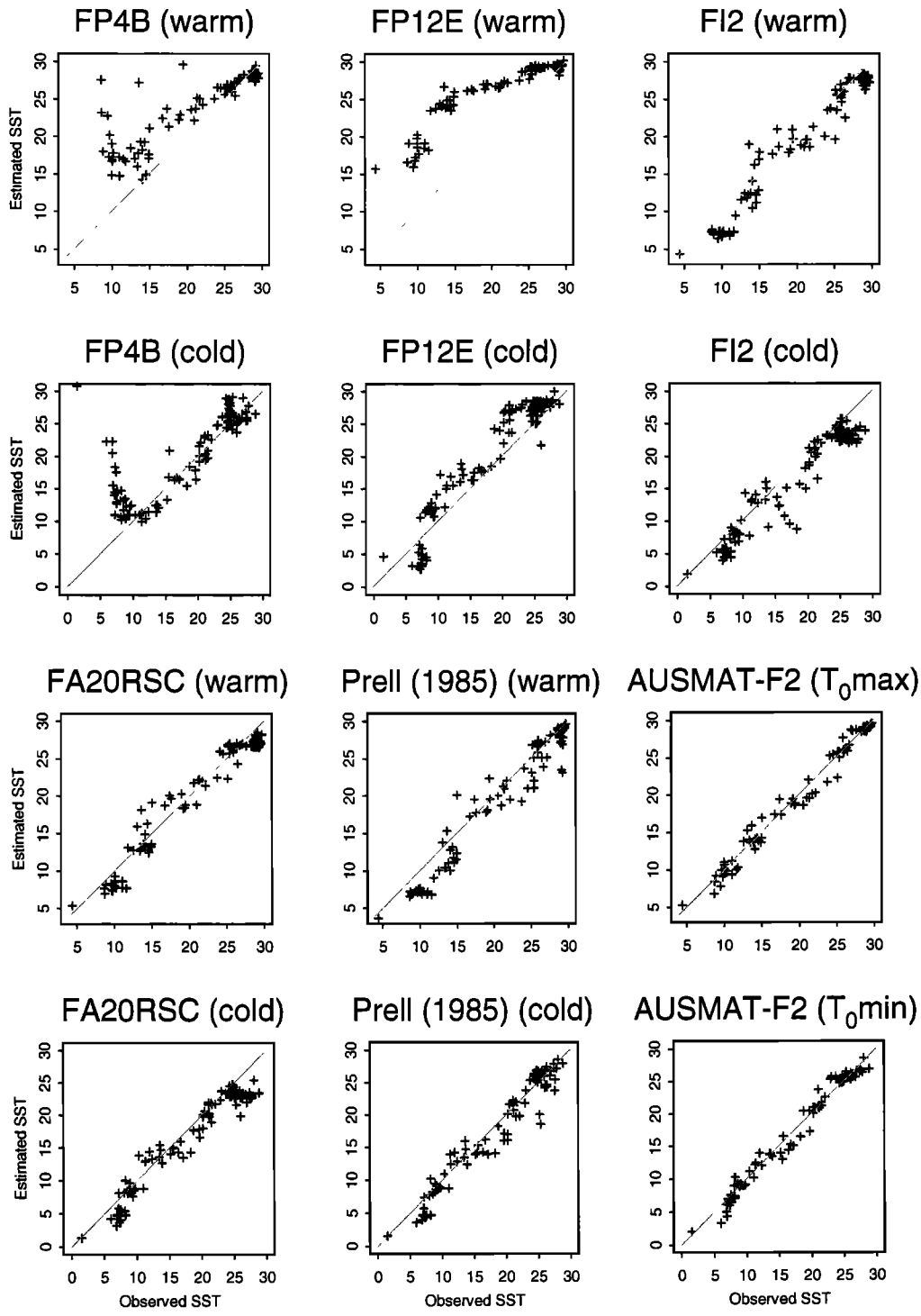

Figure 2. Observed versus estimated SST for factor-based transfer functions and the modern analog technique based on test evaluation. Observed temperatures are derived from *Levitus and Boyer* [1994].

The accuracy and precision of both factor-based and modern analog techniques are largely dependent on the quality of the modern core top samples together with their geographical, environmental, and taxonomic coverage. For example, *G. bulloides*, and *Neogloboquadrina pachyderma* (L) are both important species in the high latitudes, reaching 49% and 86% respectively, in the test database, but FP4B and FP12E lack appropriate coverage of these taxa. As a result, neither equation can adequately model assemblages with high abundances of these taxa. Similarly, the modern analog databases include

more taxa (38 varieties, including ecophenotypes in AUSMAT-F2) than FP12E, FI2, or FA20RSC. In particular, *Globigerinita quinqueloba*, a taxon that reaches 35% in the Tasman Sea [*Thiede et al.*, 1997] was not included in FP12E [*Thompson*, 1981].

Inspection of the communalities and dissimilarity measures indicates the MAT, using the AUSMAT-F2 database, outperforms all biogeography-based methods. There are three main reasons for this. First, the AUSMAT-F2 database contains more cores from the Southern Hemisphere than the *Prell* [1985] database or the transfer function calibration data sets. This means a greater coverage of both assemblage distribution and taxon responses along expanded SST gradients, resulting in a greater range of potential analogs. Indeed, the other Southern Hemisphere transfer functions not tested here, such as F1-3 of *Labracherie et al.* [1989] (49 core tops) and F81-25-5 of *Niebler and Gersonde* [1998] (81 core tops), also have a rather restricted regional coverage, and so are unlikely to outperform AUSMAT-F2. Second, the AUSMAT-F2 also excludes core tops from the northern and equatorial Atlantic and northern Pacific Oceans. The high-latitude surface current and frontal structure of these oceans is not analogous to the oceanography of the Southern Hemisphere, in addition to faunal dissimilarities (*G. ruber* (pink variety) is endemic to the Atlantic). Third, the modern SST data used in AUSMAT-F2 are from the integrated, high-quality database from the World Ocean Atlas [*Levitus and Boyer*, 1994], digitally read from 1° x 1° grids. Most of the other techniques applied here use older, lower-quality SST databases. AUSMAT-F2 also uses the temperatures of the warmest (T_0max) and coolest (T_0min) months rather than calendar months (February and August), which are not always the seasonal extremes. On the basis of these results we conclude that MAT, used in conjunction with AUSMAT-F2, currently provides the most accurate and precise method for estimating SSTs using foramineral assemblages across the range of environments represented in the southwest Pacific Ocean.

In comparison to the biogeography-based techniques, we find that SST estimated using the isotopic composition of *G. bulloides* is systematically too cold with high error (Table 1, Appendix A). Temperatures are underestimated by up to 11°C at low temperatures, well beyond the seasonal temperature range. The *G. bulloides* equation from *Bemis et al.* [1998] was not calibrated below 15°C and these results suggest it is not applicable within the tested range. The low-light equation written for the unrelated species *O. universa* [*Bemis et al.*, 1998] produces more reasonable results with higher accuracy and lower error (Table 1), but the best results are achieved using the equation for *G. sacculifer* [*Erez and Luz*, 1983]. The latter equation has a form very similar to those equations based on the inorganic precipitation of calcite [*Bemis et al.*, 1998], suggesting that the y intercept of the *Bemis et al.* [1998] equation for *G. bulloides* is too low. A source of systematic error complicating the selection of the most appropriate equation lies in the estimation of seawater $\delta^{18}O$ from salinity, as the relationship between the two parameters is not well constrained in this region. An additional source of error could be the selective dissolution of higher-temperature calcite in the subantarctic cores. On the basis of the above results, caution needs to be exercised when using the oxygen-isotopic composition of *G. bulloides* to estimate past SST in this region.

5. Methods for LGM reconstruction

5.1. Data and Stratigraphy

This study uses the published data from 24 published cores and five unpublished records (FR1/94-GC3, E26-1, Z2108, RC08-78, and RC13-38) to calculate LGM SST (Table 2). The new faunal data used in this paper are provided in Appendix B. The sample preparation methodology used for FR1/94-GC3 and E26-1 is described by *Martinez* [1994] and the methodology for Z2108, RC08-78, and RC13-38 is the same as described by *Thiede et al.* [1997]. The 29 cores come from a range of water depths (413 - 4354 m) and cover latitudes from the tropics to the subantarctic. Cores with $\delta^{18}O$ stratigraphy and radiocarbon dates were preferentially chosen for this study, but some additional cores with downcore faunal records only were included to expand the regional coverage.

The LGM level was determined by *CLIMAP Project members* [1981] as the stratigraphic $\delta^{18}O$ maximum in oxygen-isotope curves. This was assumed to equate with maximum ice volume and be globally synchronous within the mixing time of the ocean. The $\delta^{18}O$ maximum represents event 2.2 in the SPECMAP oxygen-isotope stratigraphy, identified as the uppermost $\delta^{18}O$ maximum at the base of Termination I [*Prell et al.*, 1986]. To determine the age of the peak of the LGM in the southwest Pacific Ocean, we identified the depth of event 2.2 using benthonic (where possible) or planktonic $\delta^{18}O$ data and the level where minimum SST was calculated (Table 2). Six cores with AMS ^{14}C dates close to the LGM were chosen to calculate the age of both the $\delta^{18}O$ maximum and the SST minimum (Table 3). Ages were calculated assuming linear sedimentation rates and were calibrated using INTCAL98, assuming a ΔR of 0 [*Stuiver et al.*, 1998]. The errors in the pooled mean ages do not include propagated errors from the original measurement.

5.2 Sea-surface Temperature Reconstruction

On the basis of the results in sections 3 and 4, we applied the MAT to the faunal data (using the AUSMAT-F2 database to provide analogs) to determine SST for the LGM levels. Anomalies were calculated as the difference between the MAT results and observed modern temperatures [*Levitus and Boyer*, 1994], independent of core top values. As an additional estimate of SST, the glacial-interglacial amplitude of planktonic $\delta^{18}O$ ($\Delta\delta^{18}O$) was calculated between the maximum Oxygen Isotope Chron 2 value and the core top or the stratigraphically next highest sample. After subtraction of the ice-volume effect (assumed to be 1.1‰ for the Pacific Ocean [*Schrag et al.*, 1996]), the residual was treated simply as a temperature difference. The magnitude of the temperature difference was determined for all planktonic species by dividing the residual by the slope of the *Erez and Luz* [1983] equation, based on the results in sections 3 and 4. While this approach eliminates the need to accurately estimate modern $\delta^{18}O$ of the seawater, it introduces reliance on (1) the quality of a second sample, (2) a recent age for the interglacial sample, (3) knowledge of the ice-volume effect, and (4) the assumption that there were no local changes in the precipitation-evaporation budget.

Table 2. Stratigraphy and Site Data for Cores Used in Last Glacial Maximum Reconstruction

Core	Location	Longitude, °E	Latitude, °S	Depth, m	Benthonic sp.	Planktonic sp.	Event 2.2, cm	SST_{min}, cm	Sampling Int., cm	Sed. Rate, cm kyr^{-1}	Age Int., +/- kyr	References for $\delta^{18}O$ Data	References for Faunal Data
V24-184	Coral Sea Basin	146.20	12.87	2708	-	*G. sacculifer*	20	30	10	1.5	3.4	*Anderson et al.* [1989]	*Anderson et al.* [1989]
V24-170	Coral Sea Basin	146.88	13.52	2243	-	*G. sacculifer*	30	40	10	1.9	2.6	*Anderson et al.* [1989]	*Anderson et al.* [1989]
RC13-38	Fiji Plateau	177.10	14.52	2867	-	-	-	40	10	1.9	2.6	-	this paper
RC10-131	Coral Sea Basin	157.97	14.53	2933	-	*G. sacculifer*	40	30	10	1.5	3.4	*Anderson et al.* [1989]	*Anderson et al.* [1989]
V24-157	Coral Sea Basin	147.92	14.95	1212	-	*G. sacculifer*	30	30	10	1.5	3.4	*Anderson et al.* [1989]	*Anderson et al.* [1989]
ODP site 828	Vanuatu Trench	166.28	15.29	3087	-	*G. sacculifer*	1202	1300	21	63.1	0.2	*Martinez* [1994]	*Martinez* [1994]
V24-161	Coral Sea Basin	151.45	18.20	1670	-	*G. sacculifer*	40	50	10	2.4	2.1	*Anderson et al.* [1989]	*Anderson et al.* [1989]
RC12-113	Lord Howe Rise	163.52	24.88	2454	-	*G. sacculifer*	40	40	10	1.9	2.6	*Anderson et al.* [1989]	*Anderson et al.* [1989]
RC12-109	Lord Howe Rise	157.87	25.88	2930	-	*G. sacculifer*	40	40	10	1.9	2.6	*Anderson et al.* [1989]	*Anderson et al.* [1989]
DSDP site 588	Lord Howe Rise	161.23	26.11	1533	*Uvigerina* sp.	*G.ruber*	31	42	10	2.0	2.5	*Nelson et al.* [1993b]	*Martinez* [1994]
DSDP site 591	Lord Howe Rise	164.45	31.58	2131	*Uvigerina* sp.	*G. bulloides*	31	40	10	1.9	2.6	*Nelson et al.* [1993b]	*Martinez* [1994]
Z2108	Lord Howe Rise	161.61	33.38	1448	*Uvigerina* sp.	*G. bulloides*	46	35	10	1.7	2.9	*Nelson et al.* [1993b]	this paper
S794	Bay of Plenty	178.00	35.31	2195	-	*G. bulloides*	100	139	10	6.7	0.7	*Weaver et al.* [1998]	*Wright et al.* [1995]
DSDP site 592	Lord Howe Rise	165.44	36.47	1088	*Uvigerina* sp.	*G. bulloides*	30	31	12	1.5	4.0	*Nelson et al.* [1993b]	*Martinez* [1994]
E55-6	SW of Victoria	141.06	38.85	2346	*Uvigerina* sp.	*G. bulloides*	40	45	5	2.2	1.1	*Passlow et al.* [1997]	*Passlow et al.* [1997]
RS67-GC10	SW of Victoria	140.10	38.86	3332	-	-	-	51	9	2.5	1.7	-	*Passlow et al.* [1997]
E26-1	Challenger Plateau	168.34	40.28	914	*Uvigerina* sp.	-	30	41	16	2.0	3.9	*Hesse* [1994]	this paper
P69	Hawke Bay slope	178.00	40.40	2195	*Uvigerina* sp.	*G. bulloides*	315	450	30	21.8	0.7	*Weaver et al.* [1998]	*Weaver et al.* [1998]
DSDP site 593	Challenger Plateau	167.67	40.51	1068	*Uvigerina* sp.	*G. bulloides*	38	38	13	1.8	3.5	*Nelson et al.* [1993b]	*Martinez* [1994]
SO36-7	west of Tasmania	144.75	42.25	1085	*Uvigerina* sp.	-	66	73	5	3.5	0.6	*Lynch-Stieglitz et al.*[1994]	*Wells and Connell* [1997]
R657	north Chatham Rise	181.51	42.53	1408	*Uvigerina* sp.	*G. bulloides*	60	80	10	3.9	1.3	*Weaver et al.* [1998]	*Weaver et al.* [1998]
E36-23	East Tasman Rise	150.05	43.92	2533	-	*G. bulloides*	19	24	5	1.2	2.1	*Nees* [1994]	*Martinez* [1994]
FR1/94-GC3	East Tasman Rise	150.00	44.26	2667	-	*G. bulloides*	35	40	5	1.9	1.3	*Hiramatsu et al.* [1997]	this paper
RC08-78	Chatham Rise	184.23	44.78	1756	-	-	-	50	10	2.4	2.1	-	this paper
E27-30	South Tasman Rise	147.23	45.07	3552	-	*G. bulloides*	60	70	8	3.4	1.1	*Passlow et al.* [1997]	*Passlow et al.* [1997]
U938	Chatham Rise	179.50	45.08	2700	*Uvigerina* sp.	*G. bulloides*	81	130	19	6.3	1.5	*Weaver et al.* [1998]	*Weaver et al.* [1998]
DSDP site 594	Mernoo saddle	174.95	45.52	1204	*Uvigerina* sp.	*G. bulloides*	191	252	20	12.2	0.8	*Nelson et al.* [1993a]	*Wells and Okada* [1998]
Q200	Otago slope	172.03	46.00	1370	*Uvigerina* sp.	*G. bulloides*	34	59	8	2.9	1.3	*Weaver et al.* [1998]	*Weaver et al.* [1998]
Q585	Bollon's seamount	182.08	49.70	4354	*Uvigerina* sp.	*G. bulloides*	-	39	11	1.9	2.9	*Weaver et al.* [1998]	*Weaver et al.* [1998]

Table 3. Radiocarbon Dates

Core	Depth, cm	Species	Lab ID	AMS ^{14}C Date	$\delta^{18}O_{max}$ Level Date, ka B.P.	$\delta^{18}O_{max}$ Level Age, cal ka	SST_{min} Level Date, ka B.P.	SST_{min} Level Age, cal ka	Reference
Q858	110-115	planktonic sp.	NZA-604A	16110±210	16.1	18.6	-	-	*Fenner et al.* [1992]
ODP site 828	1099	*G. sacculifer*	NZA-2037	16420±210	17.5	20.3	18.6	21.5	*Martinez* [1994]
SO36-7	66-68	*G.bulloides*	NZA-?	17340±220	17.3	20.1	18.9	21.8	*Wells and Connell* [1997]
DSDP site 594	244-248	*G.bulloides*	NZA-?	17140±150	15.2	17.6	17.4	20.1	*Wells and Okada* [1997]
Z2108	44.5-45	*G.bulloides*	OZB-142U	22150±700	-	-	17.3	20.0	this paper
E55-6	44-45	*G.bulloides*	OZB-113	16450±120	14.6	16.9	16.8	19.5	this paper
Mean					16.1	18.7	17.8	20.6	
1 σ					1.3	1.5	0.9	1.0	

Table 4. Modern and Last Glacial Maximum sea-surface temperatures

	Modern Data				AUSMAT-F2 results									$\delta^{18}O$ Results	
Core	T_0max	T_0min	Range	T_0ann	MSCD	T_0max	wσ	T_0min	wσ	Range	ΔT_0max	ΔT_0min	ΔRange	$\Delta\delta^{18}O$	ΔT_0ann
V24-184	29.1	25.0	4.2	26.8	0.097	28.5	0.9	25.0	1.3	3.5	-0.6	0.1	-0.7	0.8	1
V24-170	29.1	25.0	4.1	26.7	0.059	28.7	0.8	24.9	1.0	3.8	-0.4	-0.1	-0.3	1.2	0
RC13-38	29.3	27.0	2.3	28.2	0.055	29.1	0.5	26.6	1.6	2.5	-0.1	-0.4	0.3	-	-
RC10-131	29.1	26.3	2.8	27.6	0.066	29.0	0.3	25.6	1.2	3.4	-0.1	-0.7	0.6	1.2	0
V24-157	29.0	25.0	3.9	26.5	0.047	29.1	0.2	25.6	1.0	3.5	0.2	0.6	-0.4	1.5	-2
ODP site 828A	29.2	26.4	2.9	27.7	0.120	28.6	1.4	25.1	2.0	3.5	-0.7	-1.3	0.6	2.1	-4
V24-161	28.6	24.6	4.0	26.1	0.060	28.6	0.9	25.1	1.4	3.5	0.0	0.5	-0.5	1.2	0
RC12-113	26.0	21.2	4.8	23.3	0.131	24.7	0.9	19.2	1.8	5.6	-1.3	-2.1	0.8	0.6	2
RC12-109	26.1	21.1	4.9	23.1	0.141	24.1	1.5	18.4	1.8	5.6	-2.0	-2.7	0.7	1.3	-1
DSDP site 588	25.6	20.7	5.0	22.8	0.208	23.0	1.0	17.8	1.0	5.1	-2.6	-2.8	0.2	0.9	1
DSDP site 591	23.4	18.3	5.1	21.1	0.182	17.8	1.7	12.4	1.3	5.4	-5.6	-6.0	0.4	1.1	0
Z2108	23.1	17.8	5.3	20.6	0.104	19.0	1.9	13.9	2.3	5.1	-4.2	-3.9	-0.2	1.0	0
S794	21.4	15.8	5.6	18.5	0.177	15.3	2.3	10.3	1.4	5.0	-6.1	-5.5	-0.5	2.1	-3
DSDP site 592	20.6	15.5	5.1	18.3	0.094	15.5	2.4	10.8	1.4	4.7	-5.1	-4.6	-0.4	1.3	-1
E55-6	17.4	13.6	3.8	15.9	0.211	15.3	2.2	10.2	1.7	5.1	-2.2	-3.4	1.3	2.2	-3
RS67-GC10	17.2	13.5	3.7	15.8	0.038	13.9	1.1	9.3	0.7	4.7	-3.3	-4.2	0.9	-	-
E26-1	18.7	13.4	5.3	16.7	0.111	15.0	2.9	10.1	1.6	5.0	-3.7	-3.3	-0.4	-	-
P69	19.2	13.5	5.7	16.2	0.135	13.8	2.2	9.1	2.1	4.7	-5.4	-4.4	-1.0	2.3	-3
DSDP site 593	18.5	13.3	5 2	16.6	0.047	13.8	1 4	9.1	0.8	4.7	-4.7	-4.2	-0.5	1.4	-1
SO36-7	16.2	12.0	4.1	14.3	0.090	12.1	2.0	8.2	1.2	3.9	-4.1	-3.8	-0.2	-	-
R657	17.5	12.3	5 2	14.8	0.138	13.5	1.4	9.3	0.8	4.1	-4.0	-2.9	-1.1	2.4	-4
E36-23	15.8	11.8	4.0	14.2	0.078	13.8	2.2	9.1	1.5	4.7	-2.0	-2.8	0.7	1.3	-1
FR1/94-GC3	15.5	11.6	3.8	13.9	0.079	12.6	2.0	8.7	1.2	4.0	-2.9	-3.0	0.1	1.7	-2
RC08-78	15.6	10.6	4.9	13.4	0.046	13.9	2.2	10.0	1.2	3.9	-1.7	-0.7	-1.0	-	-
E27-30	14.1	10.9	3.2	12.6	0.120	10.1	2.0	6.3	1.5	3.8	-4.1	-4.6	0.6	1.2	0
U938	15.0	9.8	5.2	12.6	0.057	6.0	1.0	2.7	0.9	3.3	-9.0	-7.0	-1.9	1.4	-1
DSDP site 594	13.9	8.8	5.1	12.2	0.016	4.3	0.7	1.1	0.5	3.1	-9.6	-7.6	-2.0	2.4	-4
Q200	13.4	8.6	4.8	12.1	0.023	4.3	1.2	0.9	1.2	3.4	-9.1	-7.7	-1.4	1.6	-1
Q585	11.8	7.2	4 6	10.4	0.002	4.9	0.7	1.5	0.6	3.3	-7.0	-5.7	-1.3	-	-

Abbreviations are as follows: T_0max, T_0min, warmest and coolest monthly SST (°C); T_0ann, annual mean SST (°C); range, seasonality of SST (°C); MSCD, squared chord distance to nearest analog; ΔT_0max, ΔT_0min, and ΔT_0ann, LGM temperature anomalies; wσ, weighted standard deviation of the 12 closest analogs; $\Delta\delta^{18}O$, LGM to late Holocene change in $\delta^{18}O$.

6. Results

6.1. Timing of the LGM

The age of event 2.2 was calculated to be 18.7 (± 1.5) cal ka, excluding the date from Z2108, which is the only sample where the $\delta^{18}O$ maximum precedes the SST minimum (Table 3). This age is very similar to the age of 19.0 ka for the sea level minimum during the LGM [*Bard et al.*, 1993]. The calculated age of the SST minimum level leads the $\delta^{18}O$ maximumand has a mean age of 20.6 (± 1.0) cal ka. The $\delta^{18}O$ maximumlags the SST minimum in 80% of the cores used in this study, most notably in those with high sedimentation rates. Our LGM reconstruction is based on the SST minimum at 20.6 ka, close to the age of 21 ka +/- 3 recommended by *Bard* [1999]. The age of the SST minimum was used to calculate mean postglacial sedimentation rates (Table 2) which vary from low to very high (1.2 to 63.1 cm kyr^{-1}). The length of the age interval represented by the sample used in the LGM reconstruction was approximated using the sedimentation rates and the average length of the adjacent sampling intervals (Table 2). The low temporal resolution of some cores (age interval >± 2 kyr) is due to coarse sampling together with low sedimentation rates, and SST estimates from these cores are likely to be time-averaged, minimum estimates only. The action of bioturbation may also contribute to a dampening of the amplitude of SST change in the lowest sedimentation rate cores, particularly those <2 cm kyr^{-1} [*Broecker*, 1986].

6.2. Planktonic Foraminiferal Abundances

The abundances of the ten commonest species in the late Holocene and the LGM levels are shown diagrammatically in Figure 3. The subtropical and tropical faunas (dominated by *G. ruber*, *G. sacculifer*, and *Globigerinella aequilateralis*) remained almost unchanged over time north of 20°S in the Coral Sea. The subantarctic fauna (dominated by *G. bulloides* and *G. quinqueloba*), presently most common south of the STF [*Thiede et al.*, 1997; *Weaver et al.*, 1997], invaded the Tasman Sea during the LGM. The Antarctic fauna (essentially *N. pachyderma* (L)) dominated south of 45°S during the LGM with almost monospecific samples east of the South Island of New Zealand. The temperate fauna (mainly *Globorotalia inflata*, *Globorotalia truncatulinoides* (L), and *N. pachyderma* (D)), presently characterizing the water mass between the STF and the Tasman Front [*Thiede et al.*, 1997], was spatially less important during the LGM, compressed between the northward expansion of the subantarctic and antarctic faunas and the static subtropical/tropical faunas.

6.3. The MAT-Based SST Estimates

The above faunal changes are quantified into SST estimates using the MAT in Table 4. There is a striking heterogeneity in the magnitude of cooling between the LGM across the southwest Pacific Ocean, ranging from near modern to 10°C cooler than present. With the exception of two samples, the distances to the nearest modern analogs are below 0.2, and 60% of the cores have distances <0.1, indicating the LGM samples have good analogs in the AUSMAT-F2 database. The weighted standard deviation (wσ) of the closest 12 analogs gives an indication of the reliability of each estimate and over the whole data set averages 1.4 and 1.3 for T_0max and T_0min, respectively. The SST estimates are spatially coherent within the error of the method, and local differences of only 1°-2°C occur between adjacent cores. The limiting effect of low temporal resolution on the magnitude of the SST anomaly is apparent between closely spaced cores. For example, FR1/94-GC3 and DSDP site 593 are up to 1° cooler than their lower-resolution neighbors E36-23 and E26-1. Despite this, some of the lower-resolution cores show high-amplitude SST changes (DSDP site 591 and Q585).

Our estimates from the Coral Sea and northern Tasman Sea are generally warmer than those of *Anderson et al.* [1989] owing to the MAT [*Prell*, 1985] slightly underestimating at high SST. Our temperature for SO36-7 is much warmer than that estimated by *Wells and Connell* [1997], as the FI2 underestimates SST at low temperatures. The estimates of *Weaver et al.* [1998] are generally slightly warmer than ours at low temperatures but similar otherwise. The comparison of results shown by *Wells and Okada* [1997] demonstrates the gross overestimation of SST by the FP12E equations and underestimation of SST by FI2 and produces a similar estimate to ours from the MAT [*Prell*, 1985].

The results from Table 4 are used to construct isotherm maps for the LGM in Figure 4. The isotherms were contoured to minimize extrapolation errors [*Brocolli and Marciniak*, 1996] and weighted toward the values from the cores with the highest temporal resolution and the best dating.

6.4. The $\delta^{18}O$-Based SST Estimates

The planktonic $\delta^{18}O$-based estimates of SST show trends similar to those outlined above (Table 4). The $\delta^{18}O$-based estimates suggest little to no cooling throughout the Coral and Tasman Seas, similar to that shown by *Nelson et al.* [1994], despite demonstrated faunal changes. As the $\delta^{18}O$ maximum does not always correspond to the SST minimum, these are likely to be minimum estimates only. The estimates based on *G. bulloides* show less cooling than the MAT-based estimates with the exception of R657, P69, and E55-6 (the latter two of which did not possess core tops). The estimates based on *G. sacculifer* show similar changes to the MAT-based estimates with the exception of Ocean Drilling Project (ODP) site 828A suggesting a cooling of ~4°C. This is a maximumestimate, as there was no core top and the sample came from a depth of 0.45 m below seafloor [*Martinez et al.*, 1997]. Additionally, the sample is 0.4‰ more depleted than the next highest sample, which can account for ~2°C of the cooling.

7. Discussion

7.1. Patterns of LGM Cooling

Our estimates suggest minimal cooling within the tropics, reinforcing the results obtained previously by *CLIMAP Project members* [1981], *Anderson et al.* [1989], and *Thunnell et al.* [1994]. Cores north of 20°S show negligible change within the error of the MAT. The full magnitude of the cooling is difficult to assess with the temporal resolution of the cores available, but the highest-resolution core (ODP site 828A) suggests that at least 1°-2°C of cooling occurred within the tropics. Although the vertical temperature structure of the wa-

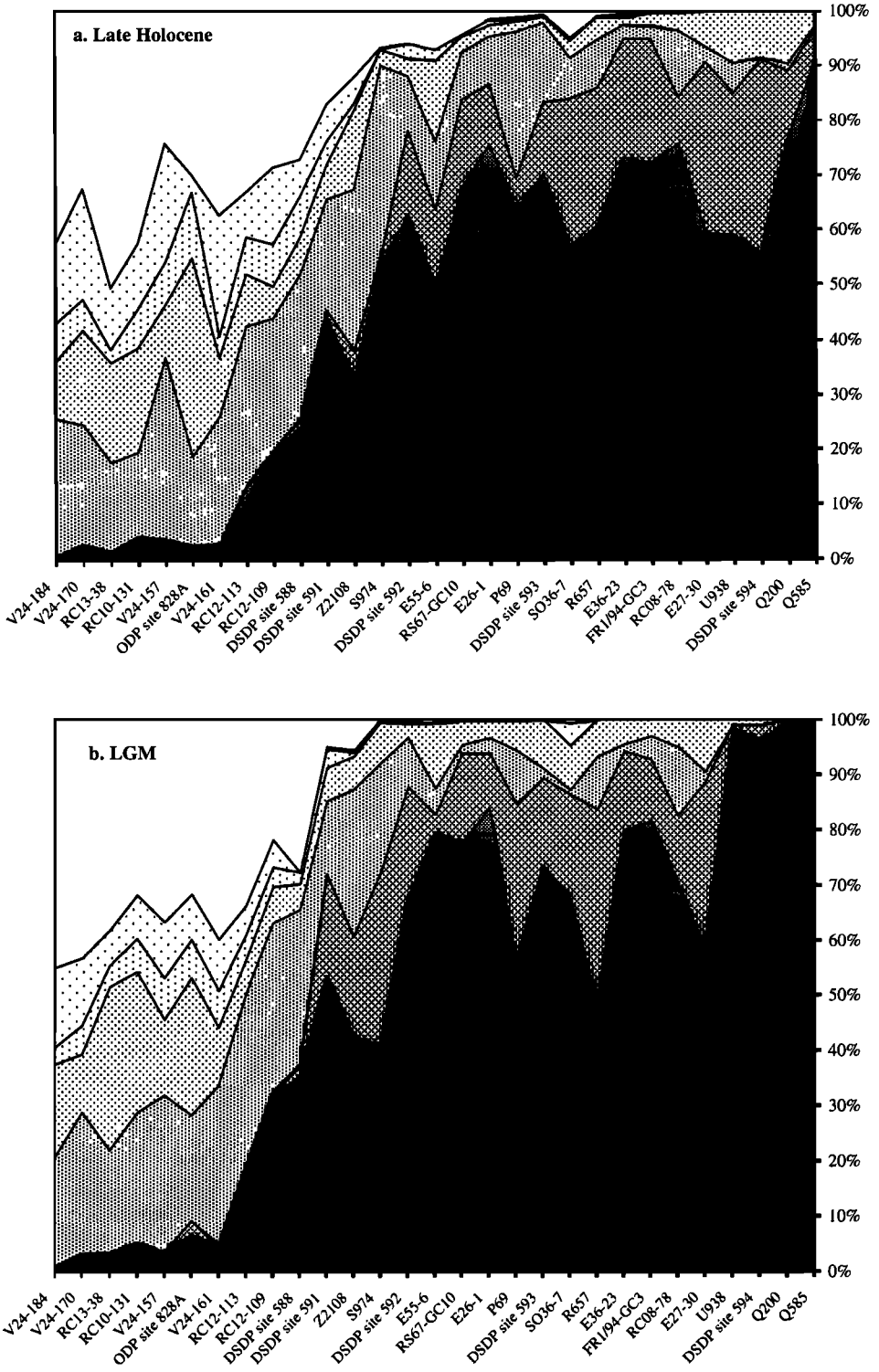

Figure 3. (a) Late Holocene and (b) Last Glacial Maximum (LGM) planktonic foraminiferal faunas for 29 cores in the southwest Pacific Ocean. Cores are ordered by latitude with the most southerly cores at the far right. For the late Holocene graph the highest stratigraphic sample was used where the core top was not available. Zonal differences in faunas are apparent, particularly in the LGM plot.

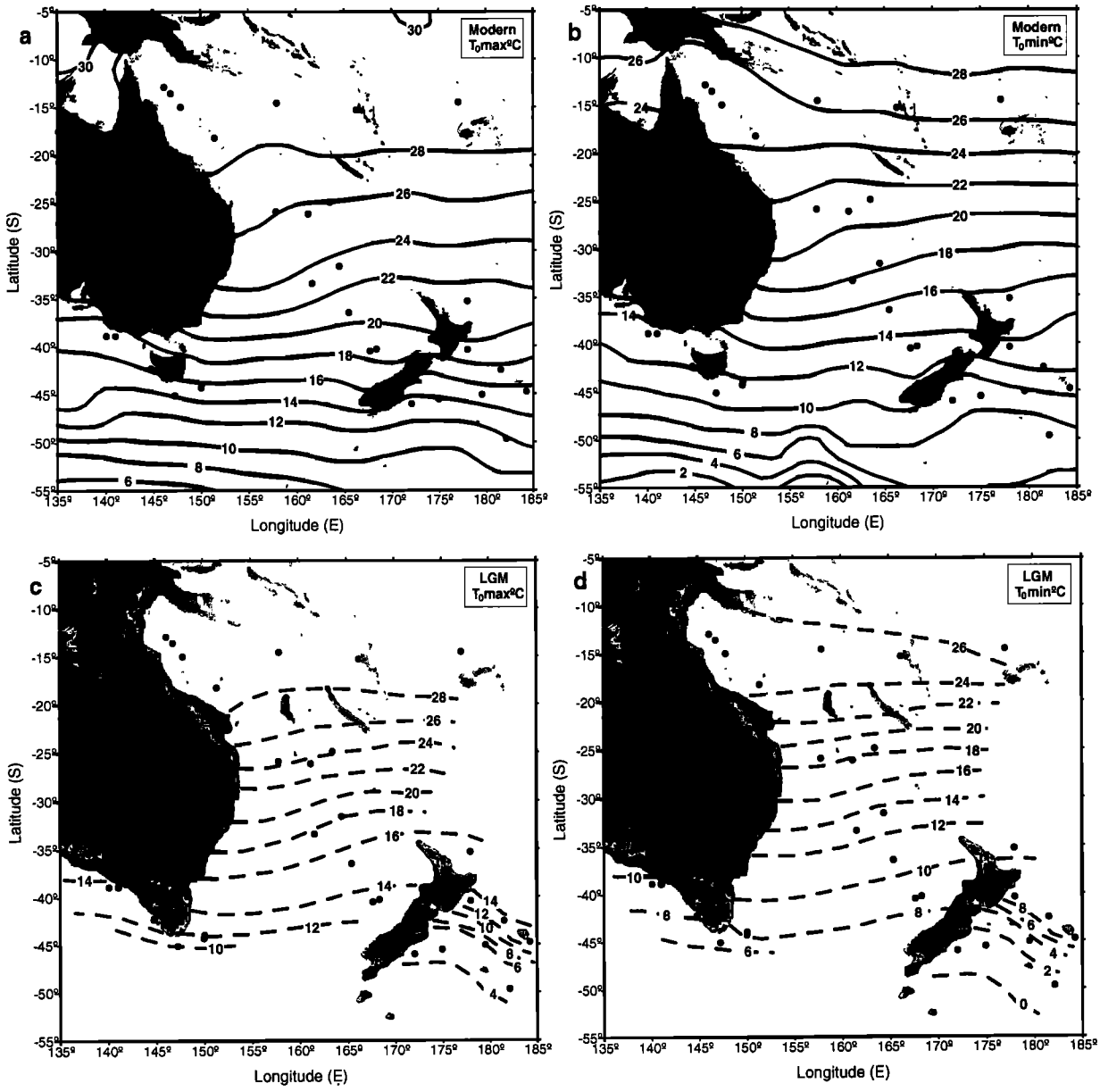

Figure 4. Sea-surface isotherms over the southwest Pacific Ocean for (a) the modern warmest month [*Levitus and Boyer*, 1994], (b) the modern coolest month [*Levitus and Boyer*, 1994], (c) the warmest month during the Last Glacial Maximum, and (d) the coolest month during the last glacial maximum. Coastline for the Last Glacial Maximum is 120 m below modern mean sea level [*Bard et al.*, 1993].

ter column explains a large amount of the distribution of tropical planktonic foraminfera [*Andreasen and Ravelo*, 1997], the faunal changes here suggest little difference in the thermocline either. As the high temperatures are reproduced in seven cores, most significantly in the core with the highest resolution (ODP-828A), the results appear to be a robust component of our reconstruction.

The northern Tasman Sea experienced a cooling of 1°-3°C. The contraction of isotherms and increased seasonalities in this area suggest a migration of the Tasman Front equatorward by ~5° of latitude, similar to that estimated by *Martinez* [1994]. It is not clear whether this is a migration as a result of shifting wind fields during the LGM or a change in the character and supply of the surface water from the Coral Sea. The magnitude of cooling increased into the middle Tasman Sea (4°-6°C) without evidence of any warm anomalies. Within the southern Tasman sea and west of Tasmania, the magnitude of cooling decreased to 2°-5°C. Modern zonal differences in SST across the southern Tasman Sea were more pronounced during the LGM, accentuated by an equatorward bowing of isotherms around New Zealand. This appears to have been caused by a cooler Tasman current along the west coast of New Zealand and a continuation of the transport of some warm water from the EAC down the east Australian coast. Isotherms presently

characterizing the STF were ~6°-7° of latitude equatorward to west of Tasmania, ~3°-6° east of Tasmania, ~7°-8° west of New Zealand and ~6°-8° east of New Zealand. The lack of significant cooling in the Tasman Sea suggested by the ^{18}O-based estimates is difficult to explain considering the large faunal changes but is most likely due to glacial differences in the ^{18}O of the seawater associated with higher salinity [*Broecker*, 1989; *Martinez et al.*, 1997]. Better understanding of the glacial precipitation-evaporation budget during the LGM and modern $\delta^{18}O$ of the seawater is needed before $\delta^{18}O$ analyses can be used to quantitatively estimate SST here.

The highest amplitude cooling (6°-10°C) occurred over the Campbell Plateau southeast of New Zealand, resulting in temperatures presently associated with the Antarctic Polar Frontal Zone. This cooling corresponds to a ~15° meriodional shift in isotherms equatorward and indicates a significant response from the Southern Ocean, displaying a similar magnitude of cooling to the North Atlantic [*CLIMAP Project Members*, 1981]. The differential cooling greatly compressed isotherms across the Chatham Rise increasing the temperature gradient to as much as 8°C over 5° of latitude [cf. *Weaver et al.*, 1998]. Evidence for the ablation of icebergs over this region is indicated by glacial erratics dredged from the Chatham Rise [*Cullen*, 1962]. Strong dissolution during the LGM in cores from the Campbell Plateau suggests the presence of a more corrosive water mass than present, which is consistent with a stronger Antarctic influence [*Weaver et al.*, 1998]. The complicating effects of the bathymetry over this region of shallow submarine plateaus makes it unclear whether the Southern Ocean fronts accompanied the isotherms into the area or whether the STF moved north off the Chatham Rise [*Weaver et al.*, 1998]. Frontal movements during the LGM will be examined elsewhere to assess the degree to which the SST response from the ocean surface was associated with changing wind fields.

Our reconstruction fills gaps in a sparsely covered region of *CLIMAP Project Members* [1981] and combines data from previous research into a single study. Our higher-precision SST estimates can be used to patch existing *CLIMAP Project Members* [1981] maps which show anomalously high temperatures over this region of the Pacific Ocean. The results from our study show that the southwest Pacific Ocean is far from a static component of the global climate with significant temperature responses in the subtropical midlatitudes as well as in the subantarctic latitudes. Despite limited temporal resolution in the tropics, our results support existing observations that the western Pacific warm pool is a relatively stable phenomenon on glacial-interglacial timescales. If surface cooling was greater in the eastern Pacific Ocean [*CLIMAP Project Members*, 1981], Walker Circulation may have been enhanced during the LGM, resulting in stronger zonal atmospheric circulation and locking the Pacific into a situation similar to the present La Niña. Such a phenomenon would explain an apparently steeper thermocline slope from east to west during the LGM [*Andreasen and Ravelo*, 1997]. Additionally, zonal atmospheric circulation could also have been vigorous because of the enhanced meridional temperature gradient produced by stronger cooling in the higher latitudes.

7.2. Land-Surface Cooling on Adjacent Landmasses

Our reconstruction supports the existing contrast between minimal cooling at the sea surface and greater cooling at high elevations on nearby island of New Guinea [*Anderson et al.*, 1989; *Thunell et al.* 1994]. The equilibrium-line altitudes (ELA) of glaciers in New Guinea were ~1000-1100 m lower than present during the LGM, approximating to a temperature difference of 5°-6°C [*Löffler*, 1982]. This temperature depression is significant at low latitudes where incident solar radiation is high. Similar magnitudes of cooling to that experienced in New Guinea look unlikely in the Coral Sea. A 6°C cooling would require a meridional shift in isotherms of more than 15° in latitude into the tropics, well beyond what is observed in the Tasman Sea. The apparent difference in cooling does not appear to be due to a large-amplitude systematic error, as we have shown a good empirical relationship between foraminiferal assemblages and SST in the modern environment and our statistics indicate that good analogs exist for the LGM conditions. It is important to note that the 6.5°C cooling reconstructed by *Beck et al.* [1997] for a coral that grew long after the LGM (10,340 ^{14}C years B.P.) is well beyond the observed shift in faunas and $\delta^{18}O$ record of core ODP site 828A in the Vanuatu Trench [*Martinez et al.*, 1997].

Contrasting with the tropics, the middle Tasman Sea shows considerable cooling at the sea surface (4°-6°C) which coincides with the latitudes of Australia where the greatest land-surface LGM cooling is recorded. *Galloway* [1965] used the periglacial limit to estimate that inland southeastern Australia (~36°S) was ~9°-11°C colder than present but found the ELA lowered by only ~800 m in SE Australia because of a reduction in precipitation. This estimate is very similar to an independent study by *Miller et al.* [1997], who used amino-acid racemization data to estimate that temperatures in central Australia (~29°S) were at least 9°C colder during the last glaciation. A pattern also exists in the southern Tasman Sea where there is moderate sea-surface cooling (2°-5°C), and terrestrial evidence in adjacent Tasmania suggests that cooling was more subdued than subtropical Australia. *Galloway* [1965] estimated that central western Tasmania was ~5°-7.5°C colder than present during the LGM, whereas an ELA depression of ~1000 m in the West Coast Range of Tasmania corresponds to a temperature drop of ~6.5°C [*Colhoun*, 1985]. The cooling on the land surface in all areas around Australia is greater than that observed in the adjacent seas.

The pattern is less clear on the eastern side of the Tasman Sea. Sea-surface cooling adjacent to the middle of New Zealand ranged from 3°-5°C. This compares to an ELA depression of ~800-850 m in the southern part of the North Island of New Zealand in central South Island, which is equivalent to at least ~4°-5°C of cooling [*Porter*, 1975; *Soons*, 1979; *Pillans et al.*, 1993]. This estimate is a minimum only, as it was also drier during the LGM in these areas [*Soons*, 1979], and reconstructions based on the Kawakawa tephra are also likely to be minimum estimates, as the eruption of this tephra preceded the SST minimum by ~5 cal kyr [*Pillans et al.*, 1993]. The magnitude of cooling at the land surface is less certain along the southern margin of New Zealand where the greatest SST cooling occurred, but Fiordland on the southwest coast of New

Zealand was extensively glaciated during the LGM [*Suggate*, 1990].

Some of the apparent differences in land-surface and sea-surface cooling outlined above may be due to biases in the records. First, most of the biases concerning the LGM levels in the marine record act to minimize the SST amplitude. Most of the deep-sea cores used here were routinely sampled at 5-10 cm intervals, resulting in only 10-20% of the information from the core being recovered. Additionally, many have low sedimentation rates and are probably bioturbated. As a result, the sediment recording the maximum cooling may not have been sampled in all cores and the signal recovered may be integrated over a long period. On this basis, it is unsurprising that the maximum cooling is seen in the highest-resolution cores. Second, geological evidence for glaciation is usually biased toward the maximum cooling, as earlier moraines are overidden or obliterated during the maximum advance. If a maximum glacial advance at full glacial conditions was a geologically brief event, lasting several hundred years, such as the Little Ice Age during the last millenium [*Broecker and Denton*, 1990], then it is probable that the event was not recorded in many of our samples because of the biases outlined above. Additionally, moraine sequences are notoriously difficult to date; so some lower-elevation moraines may relate to periods not strictly equivalent to the LGM. However, the above biases do not extend to the terrestrial records based on amino-acid racemization [*Miller et al.*, 1997] or to the deep-sea records with very high sedimentation rates [*Martinez et al.* 1997]. An additional problem concerns the synchroneity of maximum temperature depression on land versus the sea due to the observation that the SST minimum leads the $\delta^{18}O$ maximum by 2 kyr. This indicates either that the greatest sea-surface cooling preceded the maximum extent of the terrestrial ice-sheets, mainly located in the Northern Hemisphere, or that there was a lag in mixing the maximum $\delta^{18}O$ enrichment signal through the global ocean because of slower thermohaline circulation than present.

The differences in land-surface and sea-surface cooling outlined above reveal two important patterns: (1) there is a remarkably uniform depression of ELAs (800 - 1100 m) across a wide range of elevations and latitudes in the southwest Pacific Ocean, and (2) sea-surface cooling from the tropics to the subantarctic latitudes appears to be less than adjacent land-surface cooling. The first pattern suggests that planetary-scale forcing such as the greenhouse-gas content of the atmosphere, capable of acting over wide areas simultaneously, is responsible for most of the ELA lowering. Much of the variance in the temperature depression attributed to the change in ELA appears to be due to variablity in lapse rates as a result of different moisture contents in the atmosphere. The uniform lowering is particularly important considering the great latitudinal variability in sea-surface cooling demonstrated here, much of which is due to the shifting locations of surface currents. Although there is a tendency for the magnitude of the sea-surface cooling to be proportional to the land-surface cooling, the pattern implies some independence between the marine and terrestrial responses to global cooling. The second pattern suggests that the effect of global cooling is dampened at the sea surface relative to that observed on land. Although there are elevational differences between the sea surface and land surface, thermodynamic arguments have been used against the existence of steeper lapse rates during the LGM in the tropics [*Webster and Streten*, 1978]. Steeper lapse rates also cannot explain the temperature differences between the Tasman Sea and inland southern Australia, where the ~9°C cooling mentioned above occurs at close to sea level. The greater cooling in New Guinea can be somewhat accommodated through meteorological conditions allowing cold-air incursions from higher latitudes, a circulation pattern consistent with climates in Australia during the LGM [*Webster and Streten*, 1978]. In addition, up to 1°C of the difference can be accounted for by sea level depression lowering the atmospheric base. However, additional climatological arguments may need to be found to explain the differential cooling over such a large geographical area.

8. Conclusions

1. Techniques for estimating SST using planktonic foraminifera in the southwest Pacific Ocean were reviewed. The modern analog technique using the AUSMAT-F2 database produced the lowest prediction errors and had minimal bias. In addition, it was the only method applicable across the entire range of environments and assemblages tested. In comparison, provincial transfer functions written for individual oceans and the oxygen-isotope-based technique produced the highest errors.
2. An age discrepancy between the age of SST minimum (20.6 ka) and the d18O maximum(18.7 ka) was found in the southwest Pacific Ocean. This indicates either that the greatest cooling preceded the maximum terrestrial storage of ice or that there was a lag mixing the 18O enrichment signal through to this area. Reconstructions based on the isotopic maximum during Stage 2 are therefore likely to underestimate the full magnitude of cooling during the LGM in this region.
3. Sea-surface temperatures across the southwest Pacific Ocean during the LGM were reconstructed using the modern analog technique in conjunction with the AUSMAT-F2 database. Minimal cooling was found in the tropics (0°-2°C) but substantial cooling was found in the subtropical midlatitudes (3°-6°C). The greatest cooling was recorded in the subantarctic southeast of New Zealand (6°-10°C). The magnitude of cooling was found to decrease toward the equator with a maximum displacement of isotherms 15° equatorward southeast of New Zealand, 3°-8° equatorward at the Subtropical Front, and 5° equatorward at the Tasman Front. The full magnitude of cooling across much of the region, particularly the low latitudes, is still uncertain because of the low temporal resolution of many existing records.
4. The degree of cooling across the southwest Pacific Ocean was found to be generally less than that experienced on adjacent land masses, a phenomenon not exclusive to the tropics. This indicates that controls on surface cooling between land and sea during the LGM may have been sufficiently independent that similar magnitudes of cooling between the two environments are not to be expected.

Acknowledgments. We acknowledge the use of the Australian National Facility R/V Franklin to obtain core FR1/94-GC3 and ARC grants awarded to P.D.D. to fund cruise participation. The radiocarbon dates were funded from an ARC grant to P.D.D. and John Head. T.T.B. and P.D.D. benefited from a DIST grant to visit Germany to secure collaboration with J.T. Stefan Nees kindly provided access to unpublished CLIMAP data from the southwest Pacific Ocean. We also thank Dennis Cassidy from the Antarctic Core Facility, Florida State University, Tallahassee for access to the Eltanin core samples. We thank J. Marshall, J. Chappell and H. Harrison and advice on the manuscript. We also thank C. Nelson, S. Harris, and an anonymous referee for thoughtful reviews.

References

Anderson, D. M., Coral Sea Data Set, IGBP PAGES/World Data Cent-A for Paleoclimatol Data Contrib Ser. #1995-032, Natl Geophys. Data Cent Paleoclimatol Program, Boulder, Colo., 1995, http //www ngdc noaa gov.8800-/paleo/plsql/cs_search

Anderson, D M, W. L Prell, and N J. Barratt, Estimates of sea surface temperature in the Coral Sea at the last glacial maximum, *Paleoceanography, 4*(6), 615-627, 1989

Andrĕasen, D J, and A C. Ravelo, Tropical Pacific Ocean thermocline depth reconstruction for the last glacial maximum, *Paleoceanography, 12*(3), 395-413, 1997

Bard, E, Ice Age temperatures and geochemistry, *Science, 284*, 1133-1134, 1999.

Bard, E, M Arnold, R G Fairbanks, and B Hamelin, 230Th-234U and 14C dates obtained by mass spectrometry on corals, *Radiocarbon, 35*(1), 191-199, 1993

Beck, J W, J Récy, F Taylor, L Edwards, and G. Cabioch, Abrupt changes in early Holocene tropical sea surface temperature derived from coral records, *Nature, 385*, 705-707, 1997.

Belkin, I. M., and A L Gordon, Southern Ocean fronts from the Greenwich meridian to Tasmania, *J Geophys. Res., 101*(C2), 3675-3696, 1996.

Bemis, B E, H J. Spero, J Bijma, and D W Lea, Reevaluation of the oxygen isotopic composition of planktonic foraminifera Experimental results and revised paleotemperature equations, *Paleoceanography, 13*(2), 150-160, 1998.

Broccoli, A. J, and E P Marciniak, Comparing simulated glacial climate and paleodata A reexamination, *Paleoceanography, 11*(1), 3-14, 1996

Broecker, W. S, Oxygen isotope constraints on surface ocean temperatures, *Quat Res. 26*, 121-134, 1986

Broecker, W. S., The salinity contrast between the Atlantic and Pacific Oceans during glacial times, *Paleoceanography, 4(2)*, 207-212, 1989

Broecker, W. S, and G H Denton, The role of Ocean-Atmosphere reorganizations in glacial cycles, *Quat Sci Rev, 9*, 305-341, 1990

Climate Long-Range Investigation, Mapping and Prediction (CLIMAP) Project Members, The surface of the Ice-Age Earth, *Science, 191*, 1131-1137, 1976

Climate Long-Range Investigation, Mapping and Prediction (CLIMAP) Project Members, Seasonal reconstructions of the Earth's surface at the Last Glacial Maximum, *Geol Soc Am Map Chart Ser. MC-36*, 1981.

Colhoun, E A., The glaciations of the West Coast Ranges, Tasmania, *Quat. Res, 24*, 39-59, 1985

Craig, H., and L Gordon, Deuterium and oxygen-18 variation in the ocean and marine atmosphere, in *Proceedings of the 2nd Conference on Stable Isotopes in Oceanography Studies of Paleotemperature*, edited by E Tongiorgi, pp 9-130, Lab of Geol and Nucl Sci., Pisa, Italy, 1965.

Cresswell, G R, and R Legeckis, Eddies off southeastern Australia, *Deep Sea Res, Part A. 33*, 1527-1562, 1986.

Cullen, D J., The significance of a glacial erratic from the chatham Rise, east of New Zealand, *N Z. J. Geol Geophys., 5*, 309-313, 1962

Emiliani, C, Pleistocene temperatures, *J Geol, 63*, 538-578, 1955

Erez, J, and B Luz, Experimental paleotemperature equation for planktonic foraminifera, *Geochim Cosmochim Acta, 47*, 1025-1031, 1983

Fenner, J, L. Carter, and R Stewart, Late Quaternary palaeoclimatic and palaeoceanographic change over northern Chatham Rise, New Zealand, *Mar Geol., 108*, 383-404, 1992

Galloway, R. W, Late Quaternary climates in Australia, *J Geol, 73*, 603-618, 1965

Garner, D M., The Subtropical Convergence in New Zealand waters, *N Z J Geol Geophys, 2*, 315-337, 1959

Heath, R A, A review of the physical oceanography of the seas around New Zealand, *N Z. J Mar Freshwater Res, 19*, 79-124, 1985

Hesse, P. P, The record of continental dust from Australia in Tasman Sea sediments, *Quat Sci. Rev., 13*, 257-272, 1994

Hiramatsu, C, and P De Deckker, The late Quaternary nannofossil assemblages from three cores from the Tasman Sea, *Palaeogeogr Palaeoclimatol. Palaeoecol, 131*(4), 391-412, 1997.

Hutson, W H, and W. L. Prell, A paleoecological transfer function, FI-2, for Indian Ocean planktonic foraminifera, *J Paleontol, 54*(2), 381-399, 1981.

Imbrie, J, and N G Kipp, A new micropaleontological method for paleoclimatology· Application to a Late Pleistocene Caribbean core, in *The Late Cenozoic Ice Ages*, edited by K K Turekian, pp. 71-181, Yale Univ Press, New Haven, Conn 1971

Labracherie, M, L D Labeyrie, J Duprat, E Bard, M Arnold, J-J Pichon, and J-C Duplessy, The last deglaciation in the Southern Ocean, *Paleoceanography, 4*(6), 629-638, 1989

Levitus, S, and T Boyer, *World Ocean Atlas 1994*, vol. 4, *Temperature, NOAA Atlas NESDIS* 4, U S. Gov Printing Office, Wash, D C., 117 pp., 1994

Levitus, S, R Burgett, and T Boyer, *World Ocean Atlas 1994*, vol 3, *Salinity, NOAA Atlas NESDIS* 3, U S Gov Printing Office, Wash, D C., 99 pp, 1994

Löffler, E, Pleistocene and present day glaciations, in *Biogeography and Ecology of New Guinea*, vol. 1, *Monogr Biol ser*, vol 42, edited by A. Keast, pp 39-55, Dr W Junk, Norwell, Mass, 1982

Lynch-Stieglitz, J, R G Fairbanks, and C D Charles, Glacial-interglacial history of Antarctic Intermediate Water Relative strengths of Antarctic versus Indian Ocean sources, *Paleoceanography, 9*(1), 7-29, 1994.

Martinez, J. I, Late Pleistocene palaeoceanography of the Tasman Sea Implications for the dynamics of the warm pool in the western Pacific, *Palaeogeogr. Palaeoclimatol Palaeoecol, 112*, 19-62, 1994

Martínez, J I., P De Deckker, and A R. Chivas, New estimates for salinity changes in the Western Pacific Warm Pool during the last glacial maximum: oxygen-isotope evidence *Mar. Micropaleont., 32*, 311-340, 1997.

Martínez, J I., P De Deckker, and T T. Barrows, Palaeoceanography of the Last Glacial Maximum in the eastern Indian Ocean Planktonic foraminiferal evidence, *Palaeogeogr Palaeoclimatol. Palaeoecol, 147*, 73-99, 1999a

Martinez, J I., P. De Deckker, and T T Barrows, Palaeoceanography of the western Pacific warm pool during the Last Glacial Maximum - Of significance to long term monitoring of the maritime continent, in *Environmental and Human History and Dynamics of the Australian Southeast Asian Region*, edited by P Bishop, A P. Kershaw, and N Tapper, Catena Verlag, in press, 1999b.

Miller, G H, J W Magee, and A. J T. Jull, Low latitude glacial cooling in the Southern Hemisphere from amino acids in emu eggshells, *Nature, 385*, 241-244, 1997

Molfino, B, N G Kipp, and J J Morley, Comparison of foraminiferal, coccolithophorid and radiolarian paleotemperature equations Assemblage coherency and estimated concordancy, *Quat. Res, 17*, 279-313, 1982

Moore, T C Jr., et al, The reconstruction of sea surface temperatures in the Pacific Ocean of 18,000 B P, *Mar Micropaleontol., 5*, 215-247, 1980

Mulhearn, P J, The Tasman Front A study using satellite infrared imagery, *J Phys Oceanogr, 17*, 1148-1155, 1987

Nees, S, A stable-isotope record for the late Quaternary from the East Tasman Plateau, in *Evolution of the Tasman Sea Basin*, edited by G J van der Lingen, K M Swanson, and R J Muir, pp 197-201, A A. Balkema, Brookfield, Vt, 1994

Nelson, C S, P. J Cooke, C G. Hendy, and A. M. Cuthbertson, Oceanographic and climatic changes over the past 160,000 years at Deep Sea Drilling Project Site 594 off southwestern New Zealand, southwest Pacific Ocean, *Paleoceanography, 8*(4), 435-458, 1993a

Nelson, C. S., C H Hendy, and A. M Cuthbertson, Compendium of stable oxygen and carbon isotope data for the late Quaternary interval of deep-sea cores from the New Zealand sector of the Tasman Sea and southwest Pacific Ocean, *Occident Rep 16*, pp 1-87, Dep of Earth Sci. Univ. of Waikato, Hamilton, New Zealand, 1993b.

Nelson, C S, C H Hendy, and A M Cuthbertson, Oxygen-isotope evidence for climatic contrasts between Tasman Sea and Southwest Pacific Ocean during the late Quaternary, in *Evolution of the Tasman Sea Basin*, edited by G. J van der Lingen, K M Swanson, and R J Muir, pp 181-196, A A. Balkema, Brookfield, Vt, 1994

Niebler, H-S., and R Gersonde, A planktic foraminiferal transfer function for the southern South Atlantic Ocean, *Mar Micropaleontol, 34*, 187-211, 1998.

Nilsson, C S, and G R Cresswell, The formation and evolution of the East Australian Current warm-core eddies, *Prog Oceanogr, 9*, 133-183, 1981

Orsi, A H, T Whitworth, and W D Nowlin, On the meridional extent and fronts of the Antarctic Circumpolar Current, *Deep Sea Res., Part I, 42*, 641-673, 1995.

Passlow, V, W. Pinxian, and A. R Chivas, Late Quaternary palaeoceanography near Tasmania, southern Australia, *Palaeogeogr Palaeoclimatol. Palaeoecol, 131*(4), 433-463, 1997.

Pillans, B, M McGlone, A Palmer, D. Mildenhall, B. Alloway, and B Berger, The Last Glacial Maximum in central and southern North Island, New Zealand· A paleoenvironmental reconstruc-

tion using the Kawakawa tephra Formation as a chronostratigraphic marker, *Palaeogeogr. Palaeoclimatol Palaeoecol*, *101*, 1283-1304, 1993

Porter, S C, Equilibium-line altitudes of late Quaternary glaciers in the Southern Alps, New Zealand, *Quat Res*, 5, 27-47, 1975

Prell, W. L., The stability of low-latitude sea surface temperatues An evaluation of the CLIMAP reconstruction with emphasis on the positive SST anomalies, *Tech Rep. TR025*, U S Dep of Energy, Washington, D C, 1985

Prell. W. L, J Imbrie, D G Martinson, J J Morley, N G Pisias, N. J. Shackleton, and H. F Streeter, Graphic correlation of oxygen isotope stratigraphy Application to the late Quaternary, *Paleoceanography*, *1*(2), 137-162, 1986.

Rind, D, and D Peteet, Terrestrial conditions at the Last Glacial Maximum and CLIMAP sea-surface temperature estimates. Are they consistent?, *Quat Res*. *24*, 1-22, 1985

Schrag, D P, G Hampt, and D W Murray, Pore fluid constraints on the temperature and oxygen isotopic composition of the glacial ocean, *Science*, *272*, 1930-1932, 1996

Soons, J M, Late Quaternary environments in the central South Island of New Zealand *N Z. Geog.*, *35*, 16-23, 1979

Stanton, B R, The Tasman Front, *N Z J Mar Freshwater Res*, *13* (2), 201-214, 1979

Stanton, B. R, An oceanographic survey of the Tasman Front, *N Z. J. of Mar and Freshwater Res*, *15*, 289-297, 1981.

Stuiver, M, P J Reimer, E Bard, J W. Beck, G. S. Burr, K. A Hughen, B Kromer, F G. McCormac, J van der Plicht, and M Spurk, INTCAL98 radiocarbon age calibration, 24,000-0 cal BP, *Radiocarbon*, *40*(3), 1041-1083, 1998

Suggate, R P, Late Pliocene and Quaternary glaciations of New Zealand, *Quat. Sci. Rev*. *9*, 7-29, 1990

ter Braak, C J F, and S Juggins, Weighted averaging partial least squares regression (WA-PLS) An improved method for reconstructing environmental variables from species assemblages, *Hydrobiologia*, *269/270*, 485-502, 1993

Thiede, J., S Nees, H. Schulz, and P De Deckker, Oceanic surface conditions recorded on the sea floor of the southwest Pacific Ocean through the distribution of foraminifers and biogenic silica, *Palaeogeogr Palaeoclimatol. Palaeoecol*, *131*(4), 207-239, 1997

Thompson, P R, Planktonic foraminifera in the western North Pacific during the past 150,000 years Comparison of modern and fossil assemblages, *Palaeogeogr. Palaeoclimatol Palaeoecol.*, *35*, 241-279, 1981.

Thunell, R, D. Anderson, D. Gellar, and Q Miao, Sea-surface temperature estimates for the tropical western Pacific during the last glaciation and their implications for the Pacific warm pool, *Quat Res*, *41*(3), 255-264, 1994

Tomczak, M, and J S Godfrey, *Regional Oceanography: An Introduction*, 422 pp, Pergamon, Tarrytown, N. Y, 1994

Wallach, D, and B Goffinet, Mean squared error of prediction as a criterion for evaluating and comparing system models, *Ecol. Modell.*, *44*, 299-306, 1989

Weaver, P. P E., H Neil, and L Carter, Sea surface temperature estimates from the southwest Pacific based on planktonic foraminifera and oxygen isotopes, *Palaeogeogr Palaeoclimatol Palaeoecol.*, *131*(4), 241-256, 1997.

Weaver, P P. E, L. Carter, and H Neil, Response of surface water masses and circulation to late Quaternary climate change east of New Zealand, *Paleoceanography*, *13*(1), 70-83, 1998

Webster, P J, and N A Streten, Late Quaternary Ice Age climates of tropical Australia. Interpretation and reconstruction, *Quat Res*, *10*, 279-309, 1978

Wells, P E, and R Connell, Movement of hydrological fronts and widespread erosional events in the southwestern Tasman Sea during the late Quaternary, *Aust. J Earth Sci.*, *44*, 105-112, 1997

Wells, P, and H Okada, Response of nannoplankton to major changes in sea-surface temperature and movements of hydrological fronts over Site DSDP 594 (south Chatham Rise, southeastern New Zealand), during the last 130 kyr, *Mar Micropaleontol.*, *32*, 341-363, 1997

Wright, I. C, M S McGlone, C. S Nelson, and B J Pillans, An integrated latest Quaternary (stage 3 to present) paleoclimatic and paleoceanographic record from offshore nothern New Zealand, *Quat Res*, *44*, 283-293, 1995

T. T. Barrows, Research School of Earth Sciences, The Australian National University, Canberra, ACT, 0200, Australia. (Tim.Barrows@anu.edu.au)

P. De Deckker, Geology Department, The Australian National University, Canberra, ACT, 0200, Australia.

S. Juggins, Department of Geography, University of Newcastle, Newcastle upon Tyne, NE1 7RU, UK.

J. I. Martinez, Department Geología, Universidad EAFIT, Medellin, A.A. 3300, Colombia.

J. Thiede, Alfred-Wegener-Institut für Polar- und Meeresforschung, Columbusstraße, D 27568 Bremerhaven, Germany.

(Received March 11, 1999,
revised August 30, 1999;
accepted September 6, 1999.)